Major Results from Validation Tests for SMART Passive Safety Injection System with the SMART-ITL Facility

Hyun-Sik Park [a*], Hwang Bae [a], Sung-Uk Ryu[a], Jin-Hwa Yang[a], Byong-Guk Jeon[a], Yun-Gon Bang[a], Sung-Jae Yi [a]
[a]*Korea Atomic Energy Research Institute, 989-111 Daedeokdaero, Yuseong, Daejeon, 305-353, Korea*
[*]*Corresponding author: hspark@kaeri.re.kr*

1. Introduction

The Standard Design Approval (SDA) for SMART [1] was certificated in 2012 at the Korea Atomic Energy Research Institute (KAERI). To satisfy the domestic and international needs for nuclear safety improvement after the Fukushima accident, several efforts to improve its safety have been made, and a Passive Safety Injection System (PSIS) for SMART has been designed [2].

In addition, an Integral Test Loop for the SMART design (SMART-ITL, or FESTA) [3] has been constructed and it finished its commissioning tests in 2012. Consequently, a set of Design Base Accident (DBA) scenarios have been simulated using SMART-ITL. A test program to validate the performance of the SMART PSIS was launched in 2013 and its scaled-down test facility was additionally installed at the existing SMART-ITL facility. Both 1-train and 2-train PSIS validation tests have been performed during 2014 and 2015, respectively, and their results were analyzed thereafter [4, 5]. Also various thermal-hydraulic tests were performed using SMART-ITL during SMART Pre-Project Engineering (PPE). They included the full-train PSIS validation tests, safety-related tests including Design Basis Accident (DBA) scenarios, system performance tests for passive safety systems, and operation and maintenance tests [6].

In this paper, the major results from the full-train PSIS validation tests with the SMART-ITL facility will be summarized. The acquired data will be used to validate the safety analysis code and its related models, to evaluate the performance of SMART PSIS together with the Passive Residual Heat Removal System (PRHRS), and to provide base data during the application phase of the Standard Design Change Approval (SDCA) and construction licensing.

2. Methods and Results

2.1 SMART Integral Test Loop (SMART-ITL)

SMART is an integral-type reactor and thus a single pressure vessel contains all of the major components, which are the pressurizer, core, steam generator, reactor coolant pump, and so on.

SMART-ITL is scaled down using the volume scaling methodology and has all the fluid systems of SMART together with the break system and instruments, as shown in Fig. 1.

The height of the individual components is conserved between SMART and SMART-ITL. The ratio of the hydraulic diameter is 1/7, and the flow area and volume are scaled down to 1/49. The scaling ratios adopted in SMART-ITL with respect to SMART are summarized in Table 1.

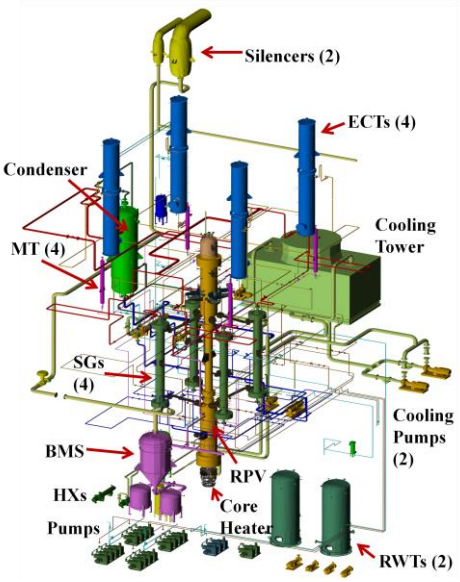

Figure 1 Schematics of the SMART-ITL.

Table 1 Major Scaling Parameters of the SMART-ITL Facility.

Parameters	Scale Ratio	Value
Length	l_{0R}	1/1
Diameter	d_{0R}	1/7
Area	d_{0R}^{2}	1/49
Volume	$l_{0R}\ d_{0R}^{2}$	1/49
Time scale, Velocity	$l_{0R}^{1/2}$	1/1
Power/Volume, Heat flux	$l_{0R}^{-1/2}$	1/1
Core power, Flow rate	$d_{0R}^{2}\ l_{0R}^{1/2}$	1/49
Pump head, Pressure drop	l_{0R}	1/1

The SMART-ITL consists of a Reactor Coolant System including a Reactor Vessel (RV), four Steam Generators (SGs), four Reactor Coolant Pumps (RCPs) to simulate asymmetric loop effects, and all passive safety systems adopted in the SMART. The secondary system, PRHRS, break system, break measuring system and auxiliary system are also installed in SMART-ITL.

All primary components except for the steam generators are equipped in a reactor pressure vessel. However, as the space of the annulus used to locate the steam generator is too narrow to install itself inside the SMART-ITL, the steam generator was connected to the

hot-leg and cold-leg outside the pressure vessel where the instruments are installed.

SMART is a 360 MW thermal power reactor, and its core exit temperature and pressurizer (PZR) pressure are 323℃ and 15 MPa during normal working conditions, respectively. The maximum power of the core heater in the SMART-ITL is 30% for the ratio of the volume scale. The reactor coolant system of the SMART-ITL was designed to operate under the same conditions as SMART.

2.2 SMART Passive Safety Injection System

The SMART PSIS design is composed of four Core Makeup Tanks (CMTs), four Safety Injection Tanks (SITs), and two-stage Automatic Depressurization Systems (ADSs) [2]. Individual tanks are connected with the pressure-balanced pipes on the top side and injection pipes on the bottom side. This system is operated when a small break loss of coolant accident (SBLOCA) or the steam line break (SLB) occurs. There are no active pumps on the pipe lines to supply the coolant. This system is only actuated by the passive means of gravity force caused by the height difference because all of the tanks are higher than the injection nozzle around the RCPs.

The CMTs and SITs were designed based on the volume scale methodology, which is the same methodology used for SMART-ITL. Their heights are conserved, their diameters are scaled down to 1/7, and the area of the tank cross-section is scaled down to 1/49. Detailed scaled values are shown in Table 1.

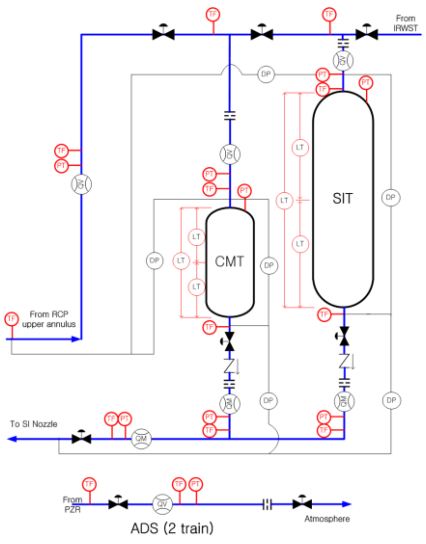

Figure 2 Schematic of the Test Facility for SMART PSIS

Fig. 2 shows a schematic of one train for the passive safety system of the SMART-ITL. Each pipe has an isolation valve and a flow meter. The pressure, differential pressure, and temperature can be measured at every pipe and tank. The level and pressure transmitters are installed in each tank.

The phenomena of flashing, condensation, and thermal stratification are expected to occur in the CMT, SITs, and pipes during the early stage. Appropriate thermo-couples have to be installed in the pipes and tanks to investigate the complex thermal-hydraulic phenomena after the system is operated by opening the isolation valve in the injection line.

Table 2 Test Matrix of full-Train SMART PSIS Tests.

Case	Break (inch)	CMT Trains	SIT Trains	Description	1-& 2-Tr. Test ID
F101	2	1, 2, 3	-	CMT only	S105 & T101
F102	2	-	1, 2, 3	SIT only	S107 & T102
F103	2	1, 2, 3	1, 2, 3	Reference case (SIS)	S108 & T103
F104	0.4	1, 2, 3	1, 2, 3	Break size effect	S110 & T104
F301	2	1, 2, 3	1, 2, 3	Break at PSV line	NA

2.3 Full-Train Validation Tests for SMART PSIS

The objectives of this research are to construct a scaled-down test facility, to assess the performance of the CMTs, SITs and ADSs for SMART, and to analyze the thermal-hydraulic phenomena of flashing, wall film condensation, interfacial direct contact condensation, and thermal stratification expected to occur inside of the tank [7-9].

An experimental facility design for validating the SMART PSIS was introduced. Through the validation tests using 1-train and 2-train PSIS, the general thermal-hydraulic performance of the passive safety system could be understood, and the performance of the nozzle geometry of the flow distributor, break size, and tank geometry could be assessed. Thus, the obtained quantitative data could be applied to a real system design and safety analysis code. Furthermore, by analyzing the experimental data, the existing condensation models for a wall film and interfacial condensation occurring in the CMTs and SITs will be assessed.

Four trains of the SMART PSIS were simulated by attaching them to the existing SMART-ITL facility. Appropriate orifices in the pressure balancing and injection lines were chosen, and the flow distributor type was selected based on the test data. The effect of the break size on the thermal-hydraulic behavior during a SBLOCA scenario was also simulated. Table 2 shows the selected test matrix of 4-Train SMART PSIS tests. Five different kinds of tests were conducted for a SBLOCA scenario to understand the following: 1) the effects of separate CMT and SIT operation, 2) the coupling effect of the CMTs and SITs, 3) the effect of different break sizes of 2 and 0.4 inches, and 4) the effect of break location (on the SIS line or PSV line).

The passive safety injection characteristics of the SMART CMT were analyzed in detail with the test data acquired using the SMART-ITL facility, for three accident scenarios of SBLOCA with a safety injection line break (F103), a steam generator tube rupture, and a feedwater line break [10]. In addition two SBLOCA tests using SMART-ITL with different break sizes of 2 and 7/32 inches were analyzed comparatively to study the effect of the maximum and minimum mass and energy loss of the reactor coolant system (RCS) [11].

2.4 SBLOCA Scenario of SMART PSIS

Table 3 Test results of major sequence for the SBLOCA tests

Event	Trip signal and Set-point	Time after break (s)		
		F 103	F 104	F 301
Break	-	0	0	0
LPP set-point	PZR Press = P_{LPP}	744	3,235	204
Reactor trip signal - Pump coastdown - CMT Act. Signal (CMTAS)	LPP+1.1 s	745	3,236	205
Reactor trip-curve start	LPP+1.6 s	746	3,237	206
MSHP set-point	LPP+4.1 s	-	-	-
CMT injection start	CMTAS+1.1s	747	3,238	206
PRHR actuation	MSHP+1.1 s	-	-	-
PRHRS IV open	PRHRAS+ 5.0 s	754	3,245	214
FIV close MSIV/ FW close	PRHRAS+ 5.0 s	755	3,245	215
SIT injection signal (SITAS)	PZR Press = P_{SITAS}	4,282	13,231	4,127
SIT injection start	SITAS+1.1 s	4,287	13,235	4,131
ADS #1 open	CMT level < $L_{ADS\#1}$	25,569	-	24,093
ADS #2 open	SIT level < $L_{ADS\#2}$	-	-	-
Test stop	-	301,258	266,342	261,326

A SBLOCA scenario was simulated using the SMART-ITL facility. The break type is a guillotine break, and its break location is on the safety injection system (SIS) line, which is located at the nozzle part of the RCP discharge. The thermal-hydraulic behavior occurs at the same time scale in the SMART-ITL and SMART designs because the SMART-ITL is a full-height test facility. Table 3 shows the major sequence of events for the SBLOCA simulation test.

When a SIS line in the SMART is broken, the primary system pressure decreases with the coolant discharge through the break. When the primary pressure reaches the low pressurizer pressure (LPP) set-point, the reactor trip signal is generated with a 1.1 s delay. Because a turbine trip and loss of off-site power (LOOP) are assumed to occur consequently after a reactor trip, the feedwater is not supplied and the RCP begins to coast-down. In addition, a CMT actuation signal (CMTAS) is generated coincidently with a reactor trip signal. With an additional 0.5 s delay, the control rod is inserted. When the PRHRS actuation signal is generated by the trip signal of the main steam high pressure (MSHP) 4.1 s after the LPP, the SG secondary side is connected to the PRHRS with a 5 s delay and is isolated from the turbine by the isolation of the main steam and feedwater isolation valves with a 20 s delay. CMT injection starts following CMTAS with a time delay of 300 s by opening the isolation valve installed on the injection line downstream of the CMT.

An SIT actuation signal (SITAS) is generated when the RCS pressure reaches below the SITAS setpoint, and the SIT tank is connected to the RPV with a 300 s delay when the isolation valve in the injection line downstream of the CMT is opened. The ADS #1 valve is opened as the CMT level falls below 35% of its full height, and the ADS #2 valve is opened as the SIT level falls below 23% of its full height.

The break nozzle diameter is 50.8 mm in the SMART design and the scaled-down value is 7.26 mm in the SMART-ITL for a 2.0 inch break. A 0.4 inch break is simulated using an orifice with an inner diameter of 1.45 mm in SMART-ITL.

2.5 Comparison between three full-train SMART PSIS Tests (F103, F104 and F301)

Table 3 also shows the major sequences of the F103, F104 and F301 tests. When a SIS line was broken during the F103 test, the RCS began to be depressurized. As the pressurizer pressure reached the LPP trip set-point at 744 s, the reactor trip was generated about 2 s after the LPP signal. Consequently, the reactor coolant pump started to coast down. The CMT actuation signal was generated. It was shown that the PRHRS actuation signal also occurred. The SIT was then actuated after the SITAS. The individual signal is sequentially actuated.

Figures 3 through 6 show the comparison results of F103, F104 and F301. Using these data, the effects of different break size and break locations are discussed. The major thermal-hydraulic parameters include the primary pressure, fluid temperatures in the CMTs and

SITs, the levels in the pressurizer, the CMTs and SITs, and the injection flow rate.

As shown in Fig. 3, the primary pressures have similar trends during the 2 inch break cases of F103 and F301, but it decreases very slowly during the 0.4 inch break cases of F104. The pressure trend is very similar to that expected during the typical SBLOCA scenario. The pressure fluctuation around 4,300 seconds during the F103 test is due to the injection from SITs. The pressure trend in the F301 test behaves a little earlier than that in the F103 test since the break occurs on the PSV line. The pressure trend in the F104 test shows a slower transient due to its smaller break size and the SIT started to be injected around 12,000 seconds after the reactor trip. The ADS #1 is actuated both in the F103 and F301 tests but not in the F104 test.

As shown in Fig. 4, the fluid temperatures in 3 CMTs have the similar trends during F103 and F301 after the injection is initiated from the CMTs, but they increase later and higher during the F104 test. As shown in Fig. 5, the fluid temperatures in the SITs show different trends. After the pressure balancing line is connected to the SITs during F103, F104 and F301, the temperatures increase abruptly with the SIT injection signal. The injection time is earlier and rapider during F103 and F301 than F104. There is small difference between the F103 and F301 tests. The SIT fluid temperature decreases faster in F301 than in F103 after 13,000 seconds after the reactor trip. Temperature trends in CMT and SIT were also similar in three trains.

As shown in Fig. 6, the pressurizer level decreases very rapidly as the break occurs in the F103 test. At around 25,000 seconds it shows the recovery of level with the operation ADS #1 but it is estimated to be a fault signal affected by dynamic pressure caused by the ADS discharge. In the F104 test, the pressurizer level is recovered around 130,000 seconds after the trip, which is not shown in this figure. As the PSV line is broken in the F301 test, the pressurizer pressure level increases during the initial period and then decreases. It begins to be recovered from around 15,000 seconds after the reactor trip. It also shows a level jump affected by dynamic pressure caused by the ADS discharge around 24,000 seconds.

As shown in Fig. 7, the CMT level decreases as the CMT inventory is injected into the reactor pressure vessel. The trends in the F103 and F301 tests are almost the same but the trend in the F104 test shows a delayed operation. In particular, the CMT levels are kept at certain levels without being emptied. The final level is higher in F104 than those in F103 and F301. Instead, as shown in Fig. 8, the SIT level decreases more slowly with the 0.4 inch break (F104) than with the 2 inch break (F103 & F301). Level trends in CMT and SIT were also similar in three trains.

Figure 9 show the comparison of total injection flowrates from both CMTs and SITs. The injected flow rates have similar trends during the 2 inch break cases of F103 and F301, but the injection is delayed during the F104 test. The fluctuations in the F103, F301, F104 tests at around 4,300 s, 4,100 s, and 13,200 s, respectively, are due to the start of SIT injection. During the F103 and F301 tests, there was an abrupt increase in the injection flow rate at around 25,000 seconds with the actuation of ADS #1. Flowrates in injection line were also similar in three trains but the fluctuation time were different one another.

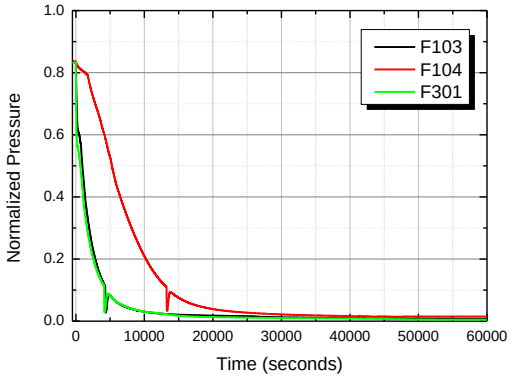

(a) CMT #1

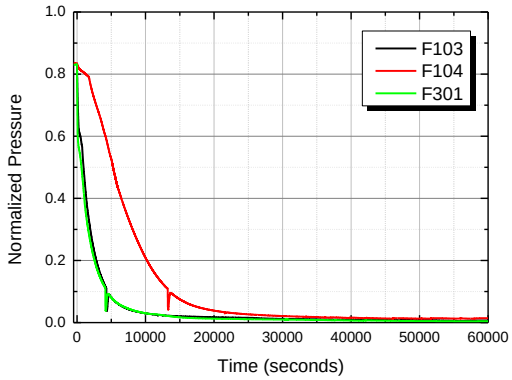

(b) CMT #2

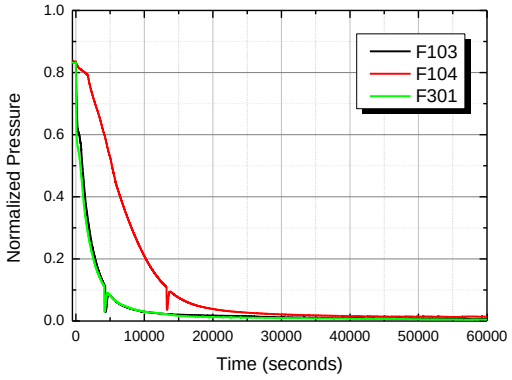

(c) CMT #3

Figure 3 Comparison of CMT pressures.

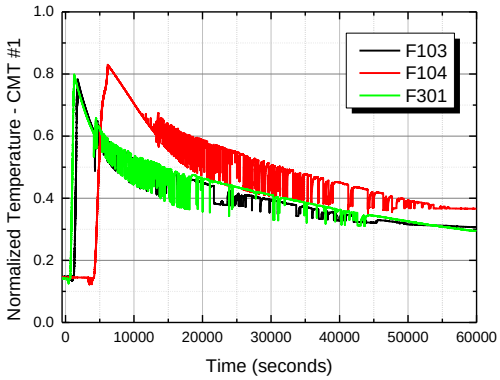

(a) Temperatures in CMT #1

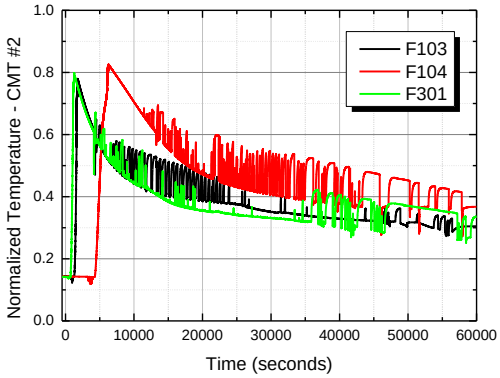

(b) Temperatures in CMT #2

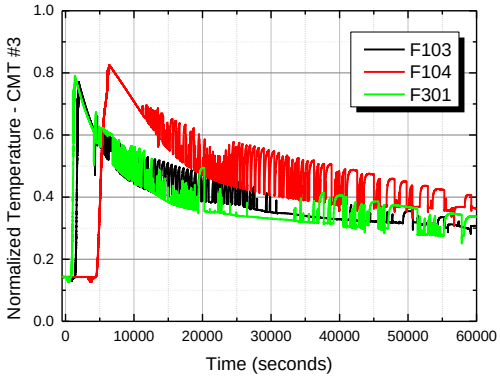

(c) Temperatures in CMT #3

Figure 4 Comparison of fluid temperatures in CMT.

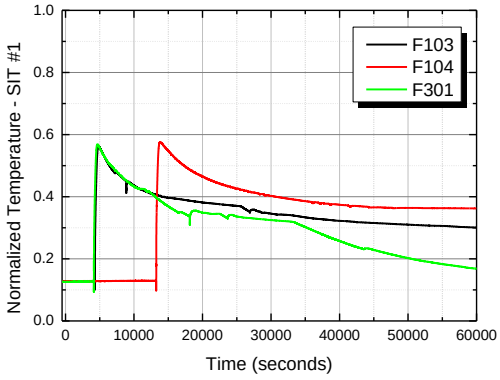

(a) Temperatures in SIT #1

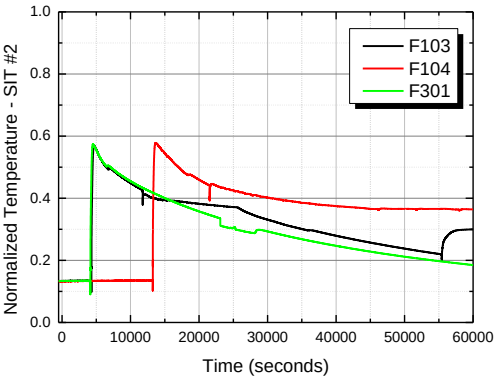

(b) Temperatures in SIT #2

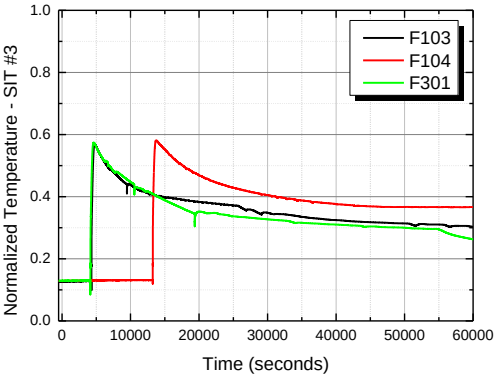

(c) Temperatures in SIT #3

Figure 5 Comparison of fluid temperatures in SIT.

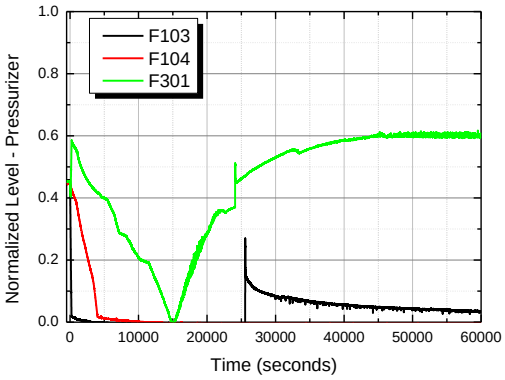

Figure 6 Comparison of levels in Pressurizer.

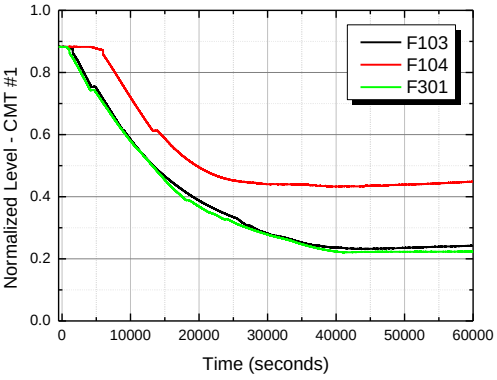

(a) CMT #1 level

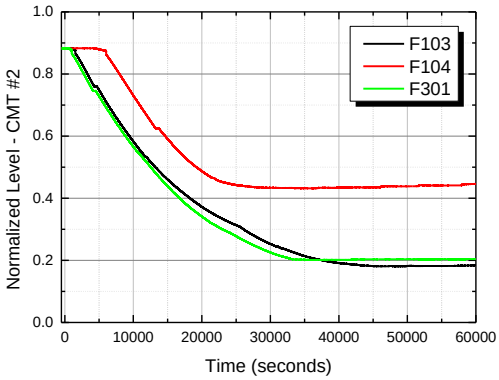

(b) CMT #2 level

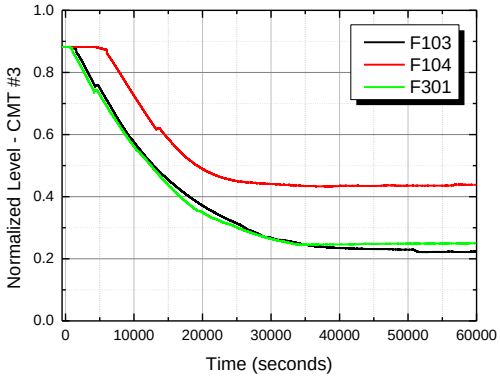

(c) CMT #3 level

Figure 7 Comparison of levels in CMT.

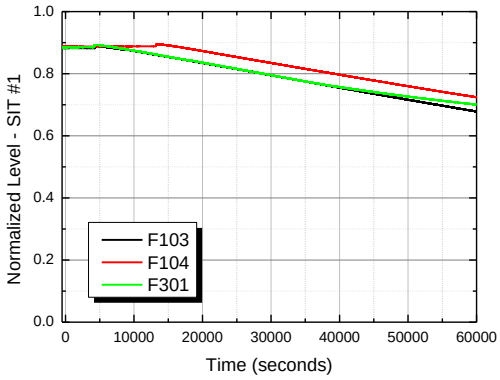

(a) SIT #1 level

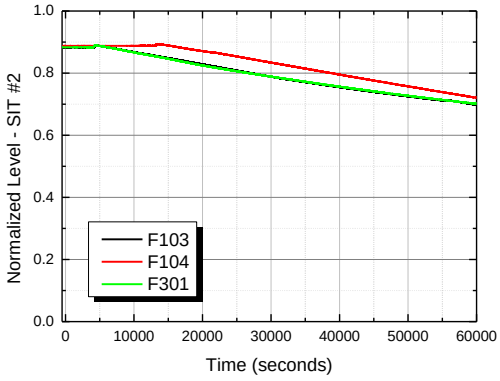

(b) SIT #2 level

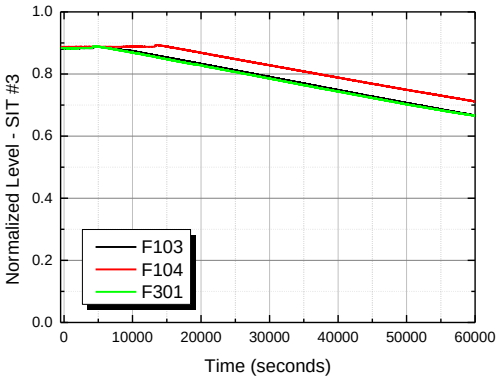

(c) SIT #3 level

Figure 8 Comparison of levels in SIT.

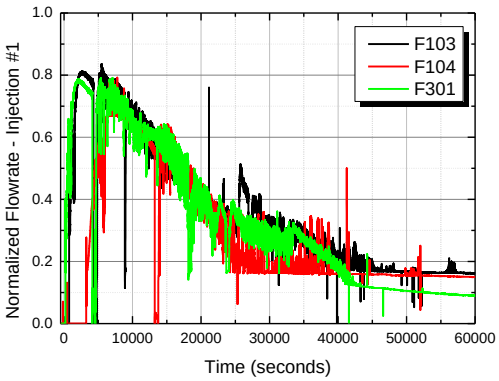

(a) Injection Line #1 (CMT+SIT)

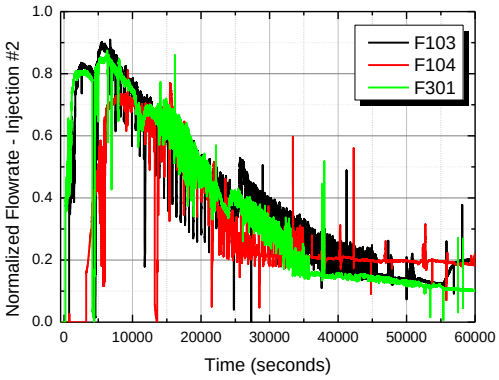

(b) Injection Line #2 (CMT+SIT)

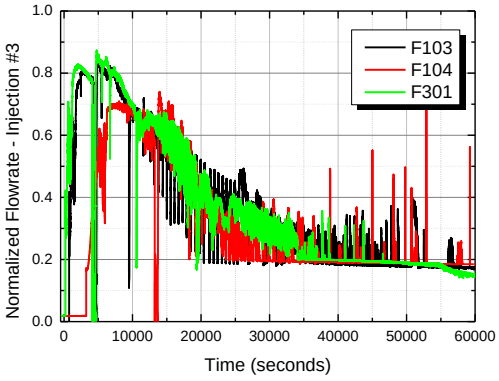

(c) Injection Line #3 (CMT+SIT)

Figure 9 Comparison of injection flowrates.

3. Conclusions

A variety of thermal-hydraulic tests were conducted to validate the performance of SMART PSIS with a scaled-down test facility of SMART PSIS, which was additionally installed at the existing SMART-ITL facility. In this paper, the major results from the SMART PSIS validation tests using the 4-trains were summarized. They included three kinds of SBLOCA tests, which are 2 inch SIS line break (F103), 0.4 inch SIS line break (F104) and 2 inch PSV line break (F301), using 4 trains of PSIS and PRHRS.

From the test results, it was estimated that the SMART PSIS had sufficient cooling capability to deal with the SBLOCA scenario of the SMART design together with PRHRS. During the SBLOCA scenario, the water inventory was well stratified thermally both in the CMTs and SITs, and the safety injection water from CMTs and SITs was injected efficiently into the RPV from the initial period, and cools down the RCS properly throughout the whole accident period.

ACKNOWLEDGEMENT

This work was supported by the SMART Standard Design Change Approval Project funded by KAERI, KHNP, and K.A.CARE.

REFERENCES

[1] K. K. Kim, et al., SMART: The First Licensed Advanced Integral Reactor, *Journal of Energy and Power Engineering*, 8, 94-102, 2014.
[2] Y. M. Bae, et al., Report of Passive Safety System, SER-410-FS403-SD, KAERI Internal Report, 2012.
[3] H. S. Park, S. J. Yi, C. H. Song, SMR Accident Simulation in Experimental Test Loop, *Nuclear Engineering International*, November 2013, 12-15, 2013.
[4] H. S. Park, et al., Major Results from 1-Train Passive Safety System Tests for the SMRT Design with the SMART-ITL Facility, *Transactions of the Korean Nuclear Society Spring Meeting*, Jeju, Korea, May 7-8, 2015.
[5] H. S. Park, et al., 2-Train Passive Safety System Tests for the SMRT Design with the SMART-ITL Facility, *Transactions of the Korean Nuclear Society Spring Meeting*, Jeju, Korea, May 12-13, 2016.
[6] H. S. Park, et al., Thermal-Hydraulic Research Supporting the Development of SMART, *NURETH-19*, Brussels, Belgium, March 6-11, 2022.
[7] K. T. Park, et al., Assessment of MARS for Direct Contact Condensation in the Core Makeup Tank, *Journal of Computational Fluids Engineering*, 19(1), pp. 64-72, 2014.
[8] S. I. Lee, Two-Stage Scaling Methodology and Direct Contact Condensation of the Core Makeup Tank in a Passive PWR, Ph.D Thesis, KAIST, 2013.
[9] J. Tuunanen, et al., Assessment of Passive Injection Systems of ALWRs, Final Report of the European Commission 4th Framework Programme Project FI4I-CT95-0004, Technical Research Centre of Finland, 1999.
[10] H. Bae, et al., Core Makeup Tank Injection Characteristics during Different Test Scenarios using SMART-ITL Facility, Annals of Nuclear Energy, 126, 10–19, 2019.
[11] J. H. Yang, et al., Comparison of Two Different Sized Small-Break LOCAs on the Passive Safety Injection Line Using SMART-ITL Data, Nuclear Technology, 206, 1421-1435, 2020.